



Self-Assembly of [3]Catenane and [4]Catenane Based on Neutral Organometallic Scaffolds

Gui-Yuan Wu^{1*}, Hong-Juan Zhu¹, Fang-Fang Pan³, Xiao-Wei Sheng¹, Ming-Rui Zhang¹, Xianyi Zhang¹, Guangxin Yao¹, Hang Qu^{2*} and Zhou Lu^{1*}

¹Anhui Province Key Laboratory of Optoelectronic Material Science and Technology, School of Physics and Electronic Information, Anhui Normal University, Wuhu, China, ²State Key Laboratory of Physical Chemistry of Solid Surfaces, Collaborative Innovation Center of Chemistry for Energy Materials (iChEM) and College of Chemistry and Chemical Engineering, Xiamen University, Xiamen, China, ³China Key Laboratory of Pesticide and Chemical Biology of Ministry of Education, College of Chemistry, Central China Normal University, Wuhan, China

OPEN ACCESS

Edited by:

Wei Wang,
East China Normal University, China

Reviewed by:

Tangxin Xiao,
Changzhou University, China
Liu-Pan Yang,
Southern University of Science and
Technology, China
Xiao-Yu Hu,
Nanjing University of Aeronautics and
Astronautics, China

*Correspondence:

Gui-Yuan Wu
wgy@ahnu.edu.cn
Hang Qu
quhangxmu@qq.com
Zhou Lu
zhoulu@ahnu.edu.cn

Specialty section:

This article was submitted to
Supramolecular Chemistry,
a section of the journal
Frontiers in Chemistry

Received: 30 October 2021

Accepted: 16 November 2021

Published: 13 December 2021

Citation:

Wu G-Y, Zhu H-J, Pan F-F,
Sheng X-W, Zhang M-R, Zhang X,
Yao G, Qu H and Lu Z (2021) Self-
Assembly of [3]Catenane and
[4]Catenane Based on Neutral
Organometallic Scaffolds.
Front. Chem. 9:805229.
doi: 10.3389/fchem.2021.805229

Transition metal-mediated templating and self-assembly have shown great potential to construct mechanically interlocked molecules. Herein, we describe the formation of the bimetallic [3]catenane and [4]catenane based on neutral organometallic scaffolds *via* the orthogonality of platinum-to-oxygen coordination-driven self-assembly and copper(I) template-directed strategy of a [2]pseudorotaxane. The structures of these bimetallic [3]catenane and [4]catenane were characterized by multinuclear NMR {¹H and ³¹P} spectroscopy, electrospray ionization time-of-flight mass spectrometry (ESI-TOF-MS), and PM6 semiempirical molecular orbital theoretical calculations. In addition, single-crystal X-ray analyses of the [3]catenane revealed two asymmetric [2]pseudorotaxane units inside the metallacycle. It was discovered that tubular structures were formed through the stacking of individual [3]catenane molecules driven by the strong π - π interactions.

Keywords: mechanically interlocked molecules, catenane, coordination-driven self-assembly, platinum-oxygen bond, metallacycle

INTRODUCTION

[n]Catenanes are a class of mechanically interlocked molecules (MIMs) consisting of two or more macrocycles that are not covalently linked to each other (Nepogodiev et al., 1998; Evans et al., 2014). These fascinating molecules have attracted increasing attention not only because of their intriguing structures and topological importance but also as a result of their potential applications in molecular machines, biomaterials, and smart materials (Niu et al., 2009; Durolo et al., 2014; Bruns et al., 2014; Fernando et al., 2016; Sawada, et al., 2016; Wu et al., 2017; Li et al., 2020; Gao et al., 2021; Lu et al., 2021). The interactions of molecular components which assist the formation of these interlocked molecules are advantageous to improve synthetic efficiency, thereby the synthesis of catenanes oftentimes utilizes the template-directed strategy which functions through molecular recognition and/or host-guest chemistry based on non-covalent interactions (Dietrich-Buchecker et al., 2003; Hao et al., 2020). These template-directed methods, including metal/organic ligand coordination, hydrophilic/hydrophobic interactions, anion templation, donor/acceptor interaction, and radical-radical interaction templating strategies, have been developed for the preparation of various topologically intriguing [n]catenanes (Kim, 2002; Sambrook et al., 2004; Shen et al., 2021).

Over the past 3 decades, coordination-driven self-assembly has become a well-established methodology for constructing a variety of supramolecular coordination complexes (SCCs) with

well-defined shapes and sizes such as one-dimensional (1D) helices, two-dimensional (2D) polygons, and three-dimensional (3D) polyhedrons (Bhat et al., 2015; Wang et al., 2015; Chen et al., 2015; Chen and Yang 2018; Wu et al., 2018; Xiao et al., 2020; Wang et al., 2021; Wang et al., 2021). The strategy pattern is usually implemented *via* the combinatorial coordination between acceptor fragments with transition-metal and donor precursors with nitrogen/carboxylate. MIMs constructed by orthogonal or hierarchical self-assembly based on coordination-driven self-assembly and other binding motifs have attracted the increasing attention recently because of their high efficiency and strong pre-organization (Li et al., 2014; Lu et al., 2018). In 2020, we reported that the construction of the [3] catenane and molecular necklace based on the charged organometallic scaffold, by employing hierarchical self-assembly involving nitrogen–platinum coordination-driven self-assembly and Cu(I) template-directed strategy (Wu et al., 2020). It should be noted that there is another established way to construct metallacycles based on oxygen-to-platinum coordination-driven self-assembly that resulted in the formation of neutral supramolecular assemblies (Xu et al., 2016). However, the construction of novel catenanes with neutral metallacycles as main scaffolds through coordination-driven self-assembly have not been reported yet. Hence, the Cu(I)-bis(phenanthroline)s-based [2]pseudorotaxane donor fragments with dicarboxylate were a kind of excellent candidates for the oxygen-to-platinum coordination-driven self-assembly of [n]catenanes. Herein, we designed and synthesized a new 60° [2]pseudorotaxane donor ligand from the dicarboxylate linear molecular axis and a 30-membered ring with the phenanthroline unit through the Cu(I) template-directed strategy. Subsequently, the [3]catenane with the neutral rhomboid scaffold and [4]catenane with the neutral triangular scaffold were successfully obtained via the formation of oxygen-to-platinum coordination bonds from the [2] pseudorotaxane donor ligand and the corresponding di-Pt(II) acceptors, respectively.

MATERIALS AND METHODS

All solvents were dried according to standard procedures, and all of them were degassed under N₂ for 30 min before use. All air-sensitive reactions were carried out under an inert N₂ atmosphere. The ¹H and ³¹P NMR spectra were recorded on a Bruker 500 MHz spectrometer (¹H: 500 MHz; ³¹P: 202 MHz) at 298 K. The ¹H and ³¹P NMR chemical shifts were reported relative to the residual solvent signals. Coupling constants (*J*) were denoted in Hz and chemical shifts (δ) in ppm. Multiplicities were denoted as follows: s = singlet, d = doublet, m = multiplet, and br = broad. The CSI-TOF-MS spectra were acquired by using an AccuTOF CS mass spectrometer (JMS-T100CS, JEOL, Tokyo, Japan). Single crystal X-ray diffraction data were collected at room temperature on XtaLAB Synergy (Dualflex, HyPix). The X-ray single-crystal diffractometer was used to study Cu K α (λ = 1.54184 Å) micro-focus X-ray sources (PhotonJet (Cu) X-ray Source). The raw data were collected and processed by CrysAlisPro software. The structures were solved by SHELXT

with intrinsic phasing and refined on *F*² by full-matrix least-squares methods with SHELXL and OLEX2 used as GUI.

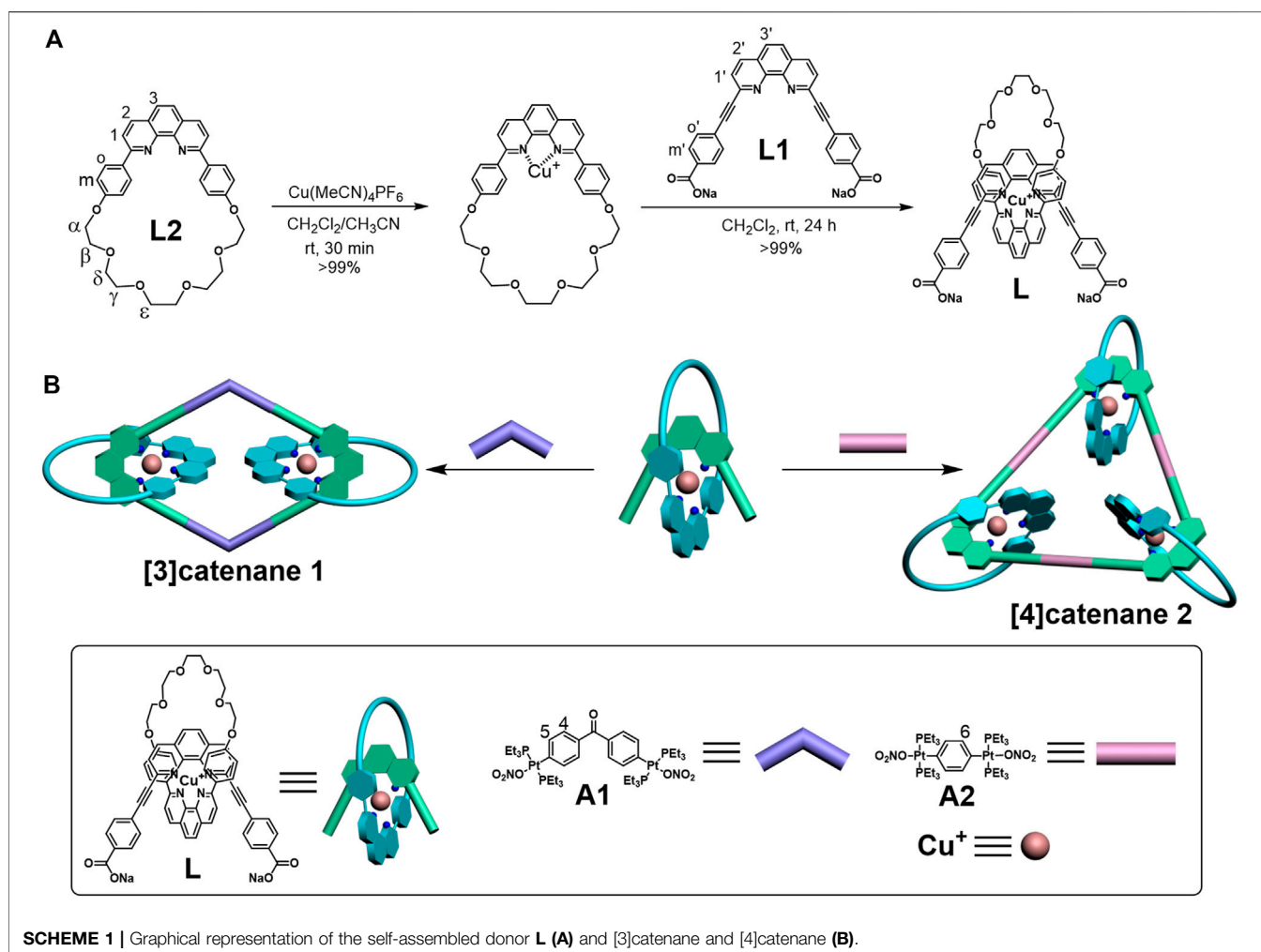
RESULTS AND DISCUSSION

Synthesis and Characterization

The hierarchical formation of the [3]catenane and [4]catenane was achieved via successive utilization of Cu(I) template-directed strategy and oxygen-to-platinum coordination-driven self-assembly (Scheme 1A). The 60° linear molecular axis L1, contained 1,10-phenanthroline (phen) and two carboxylate binding sites, can be easily synthesized according to the previous reports (Coskun et al., 2012). The [2]pseudorotaxane dicarboxylate donor L was quantitatively afforded between L1 and macrocycle L2 via the Cu(I) template-directed strategy. In a Schlenk flask, 1.0 equiv macrocycle L2 (29.47 mg, 0.052 mmol) was dissolved under nitrogen in a 20-ml (V:V = 1:1) mixture of dichloromethane and acetonitrile. After addition of 1.0 equiv Cu(MeCN)₄PF₆ (19.38 mg, 0.052 mmol), the reaction was stirred at room temperature under nitrogen for 30 min. In a second Schlenk flask, 1.0 equiv L1 (26.65 mg, 0.052 mmol) was dissolved in dichloromethane (20 ml) and cannula-filtered into the first solution. The solution was stirred under nitrogen at room temperature for an additional 24 h, followed by the removal of the solvent in vacuo to dryness to afford quantitatively L as a brown-red solid (yield = 66.29 mg, 99%). L did not obtain ¹H NMR because its solubility is very poor in organic solvents.

According to the coordination-driven self-assembly strategy, the [3]catenane **1** based on the rhomboidal scaffold was obtained by stirring donor L with an equimolar amount of a 120° di-Pt(II) acceptor A1 in a 1:7.5 ratio in H₂O/acetone at 50°C for 24 h (Figure 1) (Li et al., 2014; Wu et al., 2018; Hu et al., 2020). Similarly, the [4]catenane **2** with the triangular scaffold was formed with three [2]pseudorotaxanes L and three 180° di-Pt(II) acceptors A2 (Scheme 1B). The donor ligand L (8.85 mg, 6.87 μmol) and 120° organoplatinum acceptor A1 (8.02 mg, 6.87 μmol) were weighed accurately into a glass vial. A total amount of 3.75 ml acetone and 0.5 ml H₂O were added into the vial, and the reaction solution was stirred at 50°C for 24 h. The PF₆⁻ salt of **1** was synthesized by dissolving the NO₃⁻ salts of **1** in acetone/H₂O and adding a saturated aqueous solution of KPF₆ to precipitate the product, which was collected by vacuum filtration (yield = 15.54 mg, 99%). ¹H NMR (500 MHz, acetone-*d*₆): δ 8.81 (H₂, d, *J* = 8.2 Hz, 2H), 8.72 (H₂, d, *J* = 8.2 Hz, 2H), 8.43 (H₃, s, 2H), 8.22 (H₁, d, *J* = 8.2 Hz, 2H), 8.18 (H₃, s, 2H), 7.98 (H₁, d, *J* = 8.2 Hz, 2H), 7.66 (H₄, dd, *J* = 18.5, 7.9 Hz, 7H), 7.57 (H₅, d, *J* = 8.4 Hz, 4H), 7.43 (H₆, d, *J* = 7.9 Hz, 4H), 6.43 (H_m, d, *J* = 8.0 Hz, 4H), 6.06 (H_m, d, *J* = 8.5 Hz, 4H), 3.87 (H_e, s, 4H), 3.78–3.72 (H₈, m, 4H), 3.64–3.57 (H₇, m, 4H), 3.48 (H_{αβ}, dd, *J* = 22.4, 4.8 Hz, 8H), 1.66 (PCH₂, dd, *J* = 7.3, 3.6 Hz, 24H), 1.23 (-CH₃, dt, *J* = 15.7, 7.7 Hz, 37H). ³¹P NMR (acetone-*d*₆, 202 MHz): δ 16.51 ppm.

Following the preparation of **1** (Scheme 1), the self-assembly of the donor ligand L (9.86 mg, 7.66 μmol) with the 180° organoplatinum acceptor A2 (8.14 mg, 7.66 μmol) led to the formation of the pure [4]catenane **2** (16.53 mg, 99%). ¹H NMR (500 MHz, acetone-*d*₆): δ 8.80 (H₂, d, *J* = 8.2 Hz, 2H), 8.54 (H₂, d,



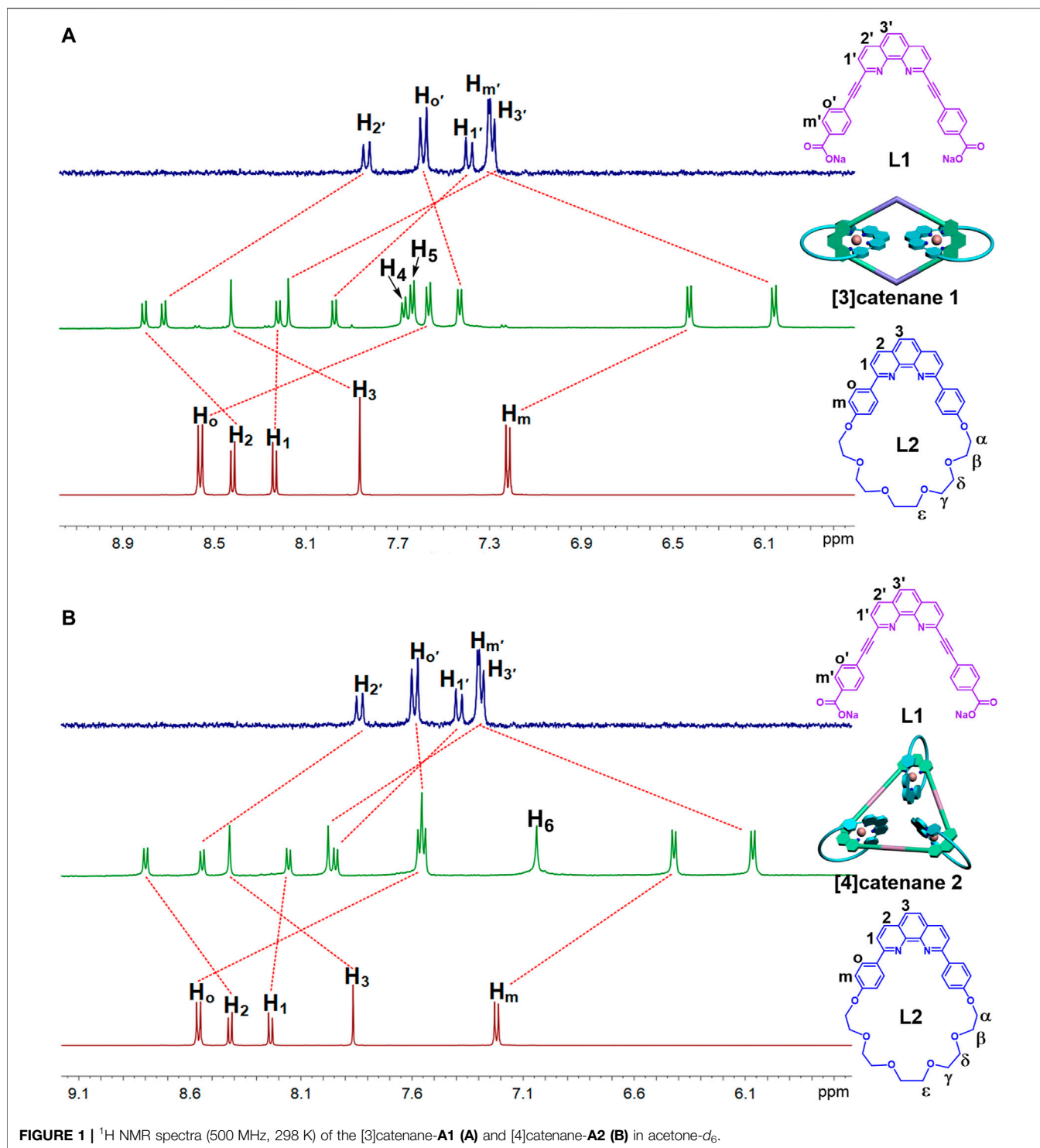
$J = 8.2$ Hz, 2H), 8.42 (H_3 , s, 2H), 8.16 (H_1 , d, $J = 8.2$ Hz, 2H), 8.02–7.90 (H_1, H_3 , m, 4H), 7.56 (H_o, H_o' , t, $J = 8.5$ Hz, 6H), 7.04 (H_6 , s, 4H), 6.42 ($H_m, d, J = 7.8$ Hz, 4H), 6.07 ($H_m, d, J = 8.3$ Hz, 4H), 3.86 (H_e , s, 4H), 3.79–3.69 (H_8 , m, 4H), 3.65–3.57 ($H_\gamma, m, 4H$), 3.48 ($H_{\alpha\beta}$, dd, $J = 22.1, 4.7$ Hz, 8H), 1.70 (PCH₂-, dd, $J = 22.7, 19.1$ Hz, 24H), 1.24 (-CH₃, ddd, $J = 30.2, 15.2, 7.2$ Hz, 36H). ³¹P NMR (acetone-*d*₆, 202 MHz): δ 16.62 ppm. ESI-MS: m/z : 2036.40 [M-3PF₆]³⁺.

Multinuclear NMR (¹H and ³¹P) analysis of the [3]catenane and [4]catenane revealed the formation of single, discrete assemblies. The most prominent features in ¹H NMR spectra of the [3]catenane **1** and [4]catenane **2** were the obvious upfield shifts of the protons (1- H_o : 8.55–7.56 ppm; 1- H_m : 7.22–6.43 ppm; 1- H_o' : 7.59–7.43 ppm; 1- H_m : 7.3–6.06 ppm; 2- H_o : 8.55–7.55 ppm; 2- H_m : 7.22–6.42 ppm; 2- H_o' : 7.59–7.55 ppm; 2- H_m : 7.3–6.06 ppm) assigned to the phen moieties, which can be explained by the two orthogonally oriented phen around the Cu(I) ion being magnetically shielded by each other (Figure 1). The ³¹P NMR spectra of [3]catenane **1** and [4]catenane **2** displayed a sharp singlet (for **1**, $\Delta\delta_{1-A1} = -2.7$ ppm; for **2**, $\Delta\delta_{2-A2} = -2.9$ ppm) that shifted upfield from the signal of the starting platinum acceptor **A1** and **A2** (Figure 2) due to the electron back-donation from the platinum atoms. In addition, the structures of the [4]catenane **2** were further confirmed by ESI-TOF-MS, which

allowed the assembly to remain intact to the maximum extent during the ionization process, while obtaining the high resolution required for isotopic distribution. For instance, the ESI-TOF-MS spectrum of **2** revealed signals that corresponded to charge states resulting from the loss of PF₆⁻ counterions, [2-3PF₆]³⁺, in which **2** represents the intact assembly (Supplementary Figure S2).

Single Crystal X-Ray Diffraction Characterization and Theoretical Calculations

The mechanically interlocked structures of the [3]catenane **1** were clearly demonstrated by X-ray crystallographic analysis (Figure 3). The single crystals of **1** were grown by slow evaporation of its dichloromethane solution. Mesomeric **1** crystallizes in the P-1 space group with two asymmetric [Cu(phen)₂]⁺ units, threading two polyether phenanthroline macrocycles onto the main Pt(II)-O-coordinated rhombic metallacycles (Figure 3A). The exterior length of **1** is approximately 2.5 nm, resulting in the large cavity with a diameter of approximately 0.8 nm. In addition, the phenyl ring of adjacent molecules exhibited the strong π - π interactions with a

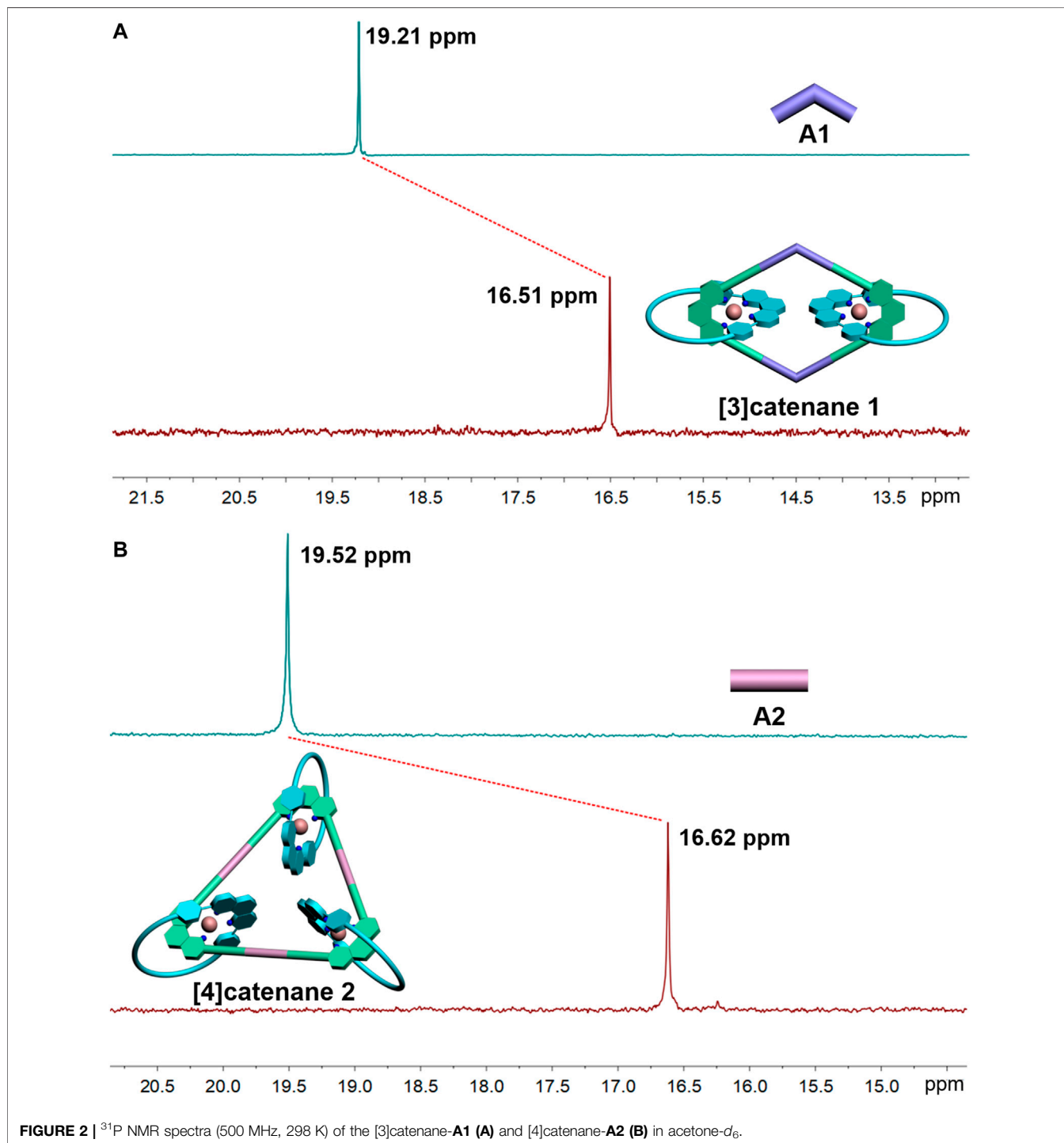


centroid-to-centroid distance of 3.86 Å (**Figure 3B**), thus leading to a liner packing of rhombic motifs and generating an interconnected 1D pore channel (**Figures 3C,D**). Thus, such kinds of catenanes based on organometallic skeletons are expected to be useful in host-guest chemistry.

To better understand the spatial structures of these catenanes, the PM6 semi-empirical quantum chemistry method (PM6-DH+) was employed to obtain the optimized geometry of the [3]catenane **1** and [4]catenane **2** (Stewart, 2007). The molecular simulation disclosed the cavity diameter of [3]catenane **1** and

[4]catenane **2** to be around 0.8 and 1.0 nm and the exterior length to be approximately 2.5 and 4.5 nm, respectively (**Figure 4**). This finding indicated that the simulation results of the [3]catenane **1** were consistent with the single crystal data. In addition, the [4]catenane based on the Pt(II)-O bonds organometallic scaffold have a relatively larger internal cavity size and exterior length than [4]catenane based on the Pt(II)-N

bonds organometallic scaffold (for the [4]catenane, cavity diameter: ca. 0.8 nm; exterior length: ca. 3.7 nm) (Wu et al., 2020). These observations were attributed to the different lengths of building blocks because the dicarboxylate donor **L1** was featured with longer length than that of the dipyridine donor in the [4]catenane based on the Pt(II)-N-bonded organometallic scaffold.



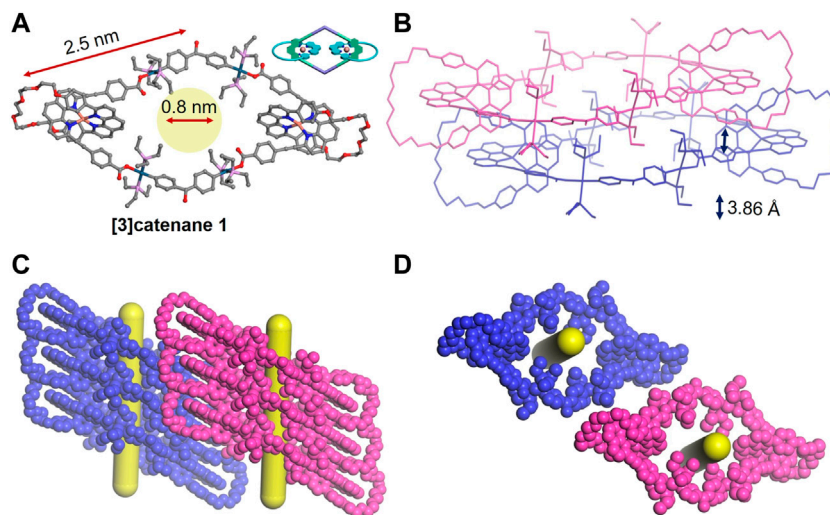


FIGURE 3 | Single-crystal structures (A), two closely packed structures (B), side view (C), and top view (D) of 3D packing structures of the [3]catenane **1**. Hydrogen atoms and PF_6^- anions are omitted for clearance.

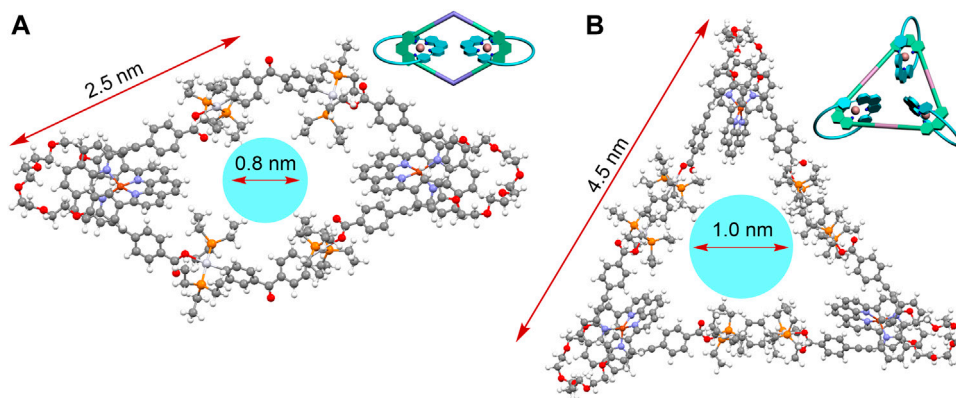


FIGURE 4 | Geometric structures of the [3]catenane **1** (A) and [4]catenane **2** (B), which were optimized at the PM6-DH + level by the semi-empirical quantum chemistry package.

CONCLUSION

In conclusion, we have shown the highly efficient construction of the [3]catenane and [4]catenane via hierarchical assembly strategy wherein oxygen-to-platinum coordination-driven self-assembly and copper(I) template-directed strategy of a 1,10-phenanthroline-based [2]pseudorotaxane comprising 30-membered rings and 60 $^\circ$ dicarboxylate donors. Multinuclear NMR $\{^1\text{H}$ and $^{31}\text{P}\}$ spectroscopy, electrospray ionization time-of-flight mass spectrometry (ESI-TOF-MS), and the PM6 semiempirical molecular orbital calculations unambiguously supported for molecular compositions. In the case of the [3]catenane, the structures of the assemblies have been established by X-ray crystallography. The crystallographic studies revealed two asymmetric $[\text{Cu}(\text{phen})_2]^+$ units inside the [3]catenane and tubular structures through the stacking of the individual [3]catenane driven by the strong π - π interactions. Such hierarchical assembly strategy,

which successively used highly efficient oxygen-to-platinum coordination-driven self-assembly and the template-directed strategy, may provide insights into the construction of other topologically complex supermolecules with well-defined structures.

DATA AVAILABILITY STATEMENT

The original contributions presented in the study are publicly available. This data can be found here: <https://zenodo.org/record/5748670#.YaiB8MiEzWE>.

AUTHOR CONTRIBUTIONS

GW conceived the project, performed most of the experiments, and analyzed the data. GW, HQ, and ZL prepared the article. HQ, FP, and

G-YW conducted single-crystal analyses. HZ and XS conducted the theoretical calculations. MZ, YH, XZ, and GY helped in experiments.

FUNDING

This work was supported by the National Natural Science Foundation of China (Nos. 21773256 and 22073001), the University Natural Science Research Project of Anhui Province

REFERENCES

- Bhat, I. A., Samanta, D., and Mukherjee, P. S. (2015). A Pd₂₄ Pregnant Molecular Nanoball: Self-Templated Stellation by Precise Mapping of Coordination Sites. *J. Am. Chem. Soc.* 137, 9497–9502. doi:10.1021/jacs.5b06628
- Bruns, C. J., and Stoddart, J. F. (2014b). Rotaxane-based Molecular Muscles. *Acc. Chem. Res.* 47, 2186–2199. doi:10.1021/ar500138u
- Chen, L.-J., Ren, Y.-Y., Wu, N.-W., Sun, B., Ma, J.-Q., Zhang, L., et al. (2015). Hierarchical Self-Assembly of Discrete Organoplatinum(II) Metallacycles with Polysaccharide via Electrostatic Interactions and Their Application for Heparin Detection. *J. Am. Chem. Soc.* 137, 11725–11735. doi:10.1021/jacs.5b06565
- Chen, L.-J., and Yang, H.-B. (2018). Construction of Stimuli-Responsive Functional Materials via Hierarchical Self-Assembly Involving Coordination Interactions. *Acc. Chem. Res.* 51, 2699–2710. doi:10.1021/acs.accounts.8b00317
- Coskun, A., Hmadeh, M., Barin, G., Gándara, F., Li, Q., Choi, E., et al. (2012). Metal-Organic Frameworks Incorporating Copper-Complexed Rotaxanes. *Angew. Chem. Int. Ed.* 51, 2160–2163. doi:10.1002/anie.201107873
- Dietrich-Buchecker, C., Colasson, B., Fujita, M., Hori, A., Geum, N., Sakamoto, S., et al. (2003). Quantitative Formation of [2]Catenanes Using Copper(I) and Palladium(II) as Templating and Assembling Centers: The Entwinning Route and the Threading Approach. *J. Am. Chem. Soc.* 125, 5717–5725. doi:10.1021/ja021370l
- Durola, F., Heitz, V., Reviriego, F., Roche, C., Sauvage, J.-P., Sour, A., et al. (2014a). Cyclic [4]Rotaxanes Containing Two Parallel Porphyrinic Plates: Toward Switchable Molecular Receptors and Compressors. *Acc. Chem. Res.* 47, 633–645. doi:10.1021/ar4002153
- Evans, N. H., and Beer, P. D. (2014). Progress in the Synthesis and Exploitation of Catenanes since the Millennium. *Chem. Soc. Rev.* 43, 4658–4683. doi:10.1039/c4cs00029c
- Fernando, I. R., Frascioni, M., Wu, Y., Liu, W.-G., Wasielewski, M. R., Goddard, W. A., et al. (2016a). Sliding-Ring Catenanes. *J. Am. Chem. Soc.* 138, 10214–10225. doi:10.1021/jacs.6b04982
- Gao, X., Cui, Z., Shen, Y.-R., Liu, D., Lin, Y.-J., and Jin, G.-X. (2021a). Synthesis and Near-Infrared Photothermal Conversion of Discrete Supramolecular Topologies Featuring Half-Sandwich [Cp*Rh] Units. *J. Am. Chem. Soc.* 143, 17833–17842. doi:10.1021/jacs.1c09333
- Hao, M., Sun, G., Zuo, M., Xu, Z., Chen, Y., Hu, X. Y., et al. (2020). A Supramolecular Artificial Light-Harvesting System with Two-Step Sequential Energy Transfer for Photochemical Catalysis. *Angew. Chem. Int. Ed.* 59, 10095–10100. doi:10.1002/anie.201912654
- Hu, Y.-X., Hao, X., Xu, L., Xie, X., Xiong, B., Hu, Z., et al. (2020). Construction of Supramolecular Liquid-Crystalline Metallacycles for Holographic Storage of Colored Images. *J. Am. Chem. Soc.* 142, 6285–6294. doi:10.1021/jacs.0c00698
- Kim, K. (2002). Mechanically Interlocked Molecules Incorporating Cucurbituril and Their Supramolecular Assemblies. *Chem. Soc. Rev.* 31, 96–107. doi:10.1039/A900939F
- (No. KJ 2020A0054), and the Natural Science Foundation of Anhui Province (No. 2108085QB79).

SUPPLEMENTARY MATERIAL

The Supplementary Material for this article can be found online at: <https://www.frontiersin.org/articles/10.3389/fchem.2021.805229/full#supplementary-material>

- Li, W.-J., Wang, W., Wang, X.-Q., Li, M., Ke, Y., Yao, R., et al. (2020). Daisy Chain Dendrimers: Integrated Mechanically Interlocked Molecules with Stimuli-Induced Dimension Modulation Feature. *J. Am. Chem. Soc.* 142, 8473–8482. doi:10.1021/jacs.0c02475
- Li, Z.-Y., Zhang, Y., Zhang, C.-W., Chen, L.-J., Wang, C., Tan, H., et al. (2014). Cross-Linked Supramolecular Polymer Gels Constructed from Discrete Multi-Pillar[5]arene Metallacycles and Their Multiple Stimuli-Responsive Behavior. *J. Am. Chem. Soc.* 136, 8577–8589. doi:10.1021/ja413047r
- Li, S., Huang, J., Zhou, F., Cook, T. R., Yan, X., Ye, Y., et al. (2014). Self-assembly of Triangular and Hexagonal Molecular Necklaces. *J. Am. Chem. Soc.* 136, 5908–5911. doi:10.1021/ja502490k
- Lu, Y., Liu, D., Lin, Y.-J., Li, Z.-H., Hahn, F. E., and Jin, G.-X. (2021b). An "All-In-One" Synthetic Strategy for Linear Metalla[4]Catenanes. *J. Am. Chem. Soc.* 143, 12404–12411. doi:10.1021/jacs.1c06689
- Lu, Y., Zhang, H.-N., and Jin, G.-X. (2018). Molecular Borromean Rings Based on Half-Sandwich Organometallic Rectangles. *Acc. Chem. Res.* 51, 2148–2158. doi:10.1021/acs.accounts.8b00220
- Nepogodiev, S. A., and Stoddart, J. F. (1998). Cyclodextrin-based Catenanes and Rotaxanes. *Chem. Rev.* 98, 1959–1976. doi:10.1021/cr970049w
- Niu, Z., and Gibson, H. W. (2009). Polycatenanes. *Chem. Rev.* 109, 6024–6046. doi:10.1021/cr900002h
- Sambrook, M. R., Beer, P. D., Wisner, J. A., Paul, R. L., Cowley, A. R., and Beer, P. D. (2004). Anion-Templated Assembly of a [2]Catenane. *J. Am. Chem. Soc.* 126, 15364–15365. doi:10.1021/ja045080b
- Sawada, T., Yamagami, M., Ohara, K., Yamaguchi, K., and Fujita, M. (2016b). Peptide [4]Catenane by Folding and Assembly. *Angew. Chem. Int. Ed.* 55, 4519–4522. doi:10.1002/anie.201600480
- Shen, Y. R., Gao, X., Cui, Z., and Jin, G. X. (2021). Rational Design and Synthesis of Interlocked [2]Catenanes Featuring Half-Sandwich Cp*Rh/Ir Units and Pyrene-Based Ligands †. *Chin. J. Chem.* 39, 3303–3308. doi:10.1002/cjoc.202100546
- Stewart, J. J. P. (2007). Optimization of Parameters for Semiempirical Methods V: Modification of NDDO Approximations and Application to 70 Elements. *J. Mol. Model.* 13, 1173–1213. doi:10.1007/s00894-007-0233-4
- Wang, H., Wang, K., Xu, Y., Wang, W., Chen, S., Hart, M., et al. (2021). Hierarchical Self-Assembly of Nanowires on the Surface by Metallo-Supramolecular Truncated Cuboctahedra. *J. Am. Chem. Soc.* 143, 5826–5835. doi:10.1021/jacs.1c00625
- Wang, W., Chen, L.-J., Wang, X.-Q., Sun, B., Li, X., Zhang, Y., et al. (2015). Organometallic Rotaxane Dendrimers with Fourth-Generation Mechanically Interlocked Branches. *Proc. Natl. Acad. Sci. U.S.A.* 112, 5597–5601. doi:10.1073/pnas.1500489112
- Wang, X.-Q., Li, W.-J., Wang, W., and Yang, H.-B. (2021). Rotaxane Dendrimers: Alliance between Giants. *Acc. Chem. Res.* 54, 4091–4106. doi:10.1021/acs.accounts.1c00507
- Wu, G.-Y., Chen, L.-J., Xu, L., Zhao, X.-L., and Yang, H.-B. (2018). Construction of Supramolecular Hexagonal Metallacycles via Coordination-Driven Self-Assembly: Structure, Properties and Application. *Coord. Chem. Rev.* 369, 39–75. doi:10.1016/j.ccr.2018.05.009
- Wu, G.-Y., Shi, X., Phan, H., Qu, H., Hu, Y.-X., Yin, G.-Q., et al. (2020). Efficient Self-Assembly of Heterometallic Triangular Necklace with

- Strong Antibacterial Activity. *Nat. Commun.* 11, 3178–3188. doi:10.1038/s41467-020-16940-z
- Wu, G.-Y., Wang, X.-Q., Chen, L.-J., Hu, Y.-X., Yin, G.-Q., Xu, L., et al. (2018). Supramolecular Polymer Cross-Linked by Discrete Tris-[2] pseudorotaxane Metallacycles and its Redox-Responsive Behavior. *Inorg. Chem.* 57, 15414–15420. doi:10.1021/acs.inorgchem.8b02712
- Wu, Q., Rauscher, P. M., Lang, X., Wojtecki, R. J., de Pablo, J. J., Hore, M. J. A., et al. (2017). Poly[N]catenanes: Synthesis of Molecular Interlocked Chains. *Science* 358, 1434–1439. doi:10.1126/science.aap7675
- Xiao, T., Zhong, W., Yang, W., Qi, L., Gao, Y., Sue, A. C.-H., et al. (2020). Reversible Hydrogen-Bonded Polymerization Regulated by Allosteric Metal Templatation. *Chem. Commun.* 56, 14385–14388. doi:10.1039/D0CC06381A
- Xu, X.-D., Yao, C.-J., Chen, L.-J., Yin, G.-Q., Zhong, Y.-W., and Yang, H.-B. (2016). Facile Construction of Structurally Defined Porous Membranes from Supramolecular Hexakistriphenylamine Metallacycles through Electropolymerization. *Chem. Eur. J.* 22, 5211–5218. doi:10.1002/chem.201504480

Conflict of Interest: The authors declare that the research was conducted in the absence of any commercial or financial relationships that could be construed as a potential conflict of interest.

Publisher's Note: All claims expressed in this article are solely those of the authors and do not necessarily represent those of their affiliated organizations, or those of the publisher, the editors, and the reviewers. Any product that may be evaluated in this article, or claim that may be made by its manufacturer, is not guaranteed or endorsed by the publisher.

Copyright © 2021 Wu, Zhu, Pan, Sheng, Zhang, Zhang, Yao, Qu and Lu. This is an open-access article distributed under the terms of the Creative Commons Attribution License (CC BY). The use, distribution or reproduction in other forums is permitted, provided the original author(s) and the copyright owner(s) are credited and that the original publication in this journal is cited, in accordance with accepted academic practice. No use, distribution or reproduction is permitted which does not comply with these terms.